

# **Solving Flight Planning Problem for Airborne LiDAR Data Acquisition Using Single and Multi-Objective Genetic Algorithms**

Ajay Dashora<sup>1</sup>, Bharat Lohani<sup>1</sup> and Kalyanmoy Deb<sup>2</sup>

<sup>1</sup>Department of Civil Engineering, <sup>2</sup>Department of Mechanical Engineering  
Indian Institute of Technology Kanpur  
PIN 208016, Uttar Pradesh, India  
{ajayd,blohani,deb}@iitk.ac.in

**Kanpur Genetic Algorithms Laboratory Report Number 2013012**

<http://www.iitk.ac.in/kangal/pub.htm>

**Abstract:** Genetic algorithms (GA) are being widely used as an evolutionary optimization technique for solving optimization problems involving non-differentiable objectives and constraints, large dimensional, multi-modal, overly constrained feasible space and plagued with uncertainties and noise. However, to solve different kinds of optimization problems, no single GA works the best and there is a need for *customizing* a GA by using problem heuristics to solve a specific problem. For the airborne flight planning problem, there is not much prior optimization studies made using any optimization procedure including a GA. In this paper, we make an attempt to devise a customized GA for solving the particular problem to arrive at a reasonably good solution. A step-by-step procedure of the proposed GA is presented and every step of the procedure is explained. Both single and multi-objective versions of the problem are solved for a particular scenario of the flight planning for airborne LiDAR data acquisition problem to demonstrate the use of a GA for such a real-world problem. The deductive approach successfully identifies the appropriate configurations of GA. The paper demonstrates how a systematic procedure of developing a customized optimization procedure for solving a real-world problem involving mixed variables can be devised using an evolutionary optimization procedure.

## **1. Introduction**

Over the past two decades, there had been remarkable developments in the field of evolutionary algorithms for solving real-world and complex optimization problems.

Genetic algorithms (GA) have been widely used for this purpose in a variety of applications. The reasons for the success of GAs in such complex problem solving tasks compared to their classical counterparts are that (i) their operators are flexible and modifiable with problem information, (ii) capable of handling mixed variables, (iii) capable of handling multi-modal problems, (iv) capable of utilizing information about uncertainties in decision variables and noise in objective and constraint value computations and (v) capable of working within restricted feasible search space.

In general, there are apparently two branches in the field of GA development and research. The first branch deals with the development of new algorithms of GA by modifying and configuring various genetic operators (i.e. selection, mutation, crossover, elite preservation etc). The developed algorithms of GA are tested against the 30 standard optimization problems. On the other hand, in the second branch of GA research, the existing algorithms are applied on the optimization problems. In some of the studies, researchers also prefer to implement the developed algorithms on the practical problems and confirm their applicability and performance. However, as GA is explored and configured specifically with an orientation to solve a particular class of problems, there is no generic set of GA algorithms, which will certainly work for all problems. As a result, there is no generic methodology available or suggested in the literature for the effective use of GA for optimization. Further, there is no literature available that compiles a complete line of framework suggesting a step-by-step procedure to solve a real-world problem wherein the nature and behaviour of the objective and constraint functions is unknown. In this paper, authors show a step-wise approach of exploration of GA that can be adopted in general to solve many different classes of problems.

The process of GA consists of three sequential steps: initialization, objective and constraints evaluation, and regeneration of new solutions. In the initialization step, population (or samples) of design vectors are generated either randomly or using some knowledge of previously known good solutions. The values of the objective and constraint functions for these population members are evaluated in the second step. Based on these function values, new population members are created using selection, crossover,

mutation and elite preservation techniques in the regeneration step. For a detail explanation and description of the genetic operators, readers can refer a book on GA by Goldberg [1] or more recent literature.

In this paper, we showcase how a generic framework of a GA can be modified to solve a complex optimization problem in systematic manner. Flight planning, which is briefly mentioned in Section 2, is one example of such complex problems. For solving any optimization problem, procedures of handling mixed variables, initialization, and elite preservation strategies are addressed in Section 3. In addition, parameter space *niching*, which helps in maintaining much-desired diversity within a GA population is also explored. The developed algorithms resulting from the combination of the various strategies of variable handling, initialization, elite preservation techniques, and parameter space *niching* are mentioned in Section 4 and investigated in Section 5 for a set of real-world problems. Further, the importance of the use of multi-objective optimization is also explained in Section 6 to develop a better understanding of the associated optimization problem. Based on the observations of the optimization process for the real-world problems, conclusions are derived in Section 7.

## 2. Flight Planning Problem

Flight planning problem for airborne LiDAR data acquisition, which is developed and discussed in detail by Dashora [2], is considered as an example of a minimization problem. The fitness function is formulated as time duration required to travel by an aircraft (or helicopter) over a given area of interest (AOI) with given characteristics of terrain for collecting the LiDAR data by means of an airborne laser scanner with navigation sensors (Global Positioning System or GPS, and Inertial Measurement Unit or IMU). Along with the LiDAR data, photographic or image data can also be collected with airborne digital camera in the same flight. The starting point of flying operation over AOI is shown by point S in Figure 1. Aircraft covers the AOI in the form of parallel strips, each of which has an effective width equal to  $B$ . After covering a flight strip, which is at flying direction  $\theta$  w.r.t.  $x$ -axis of map, the aircraft navigates back to next strip by turning. The next strip may be reached by consecutive turning mechanism, non-consecutive turning mechanism, or hybrid turning

mechanism. Consecutive turning mechanism is shown in Figure 1 below. In non-consecutive turning mechanism, aircraft turns to a non-consecutive flight strip whereas hybrid turning mechanism is a combination of consecutive and non-consecutive turning mechanisms. Once all strips are covered and data collection is completed, aircraft exits from point E.

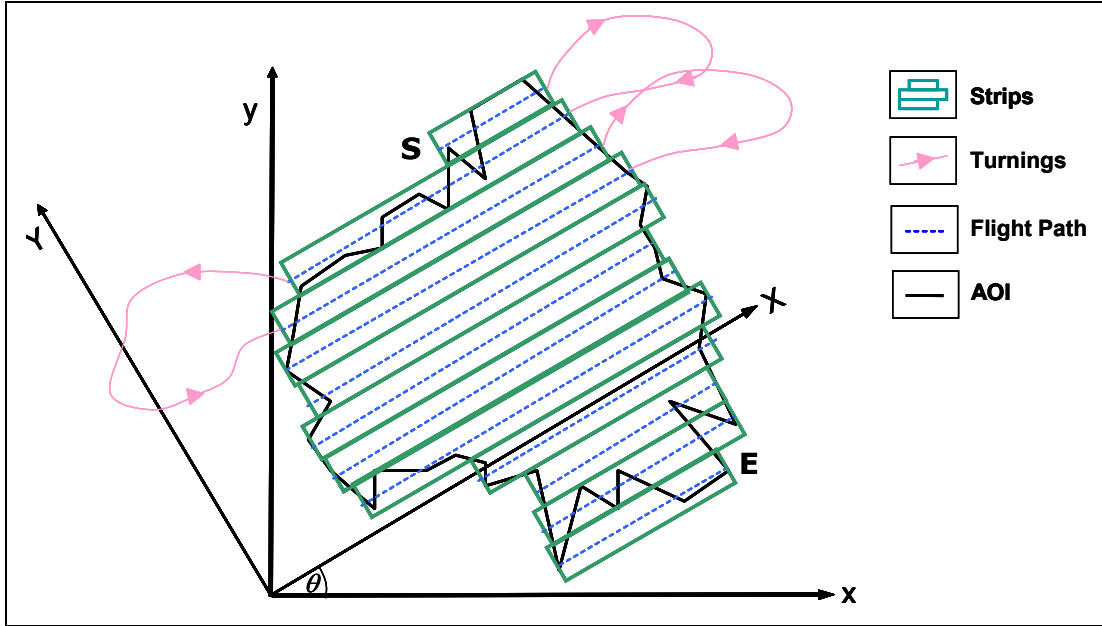


**Fig. 1: Schematic view of AOI, flight strips and turnings [2]**

The terrain surface or landscape enclosed by AOI may be flat or undulated. Similarly, airborne LiDAR data can be captured with or without photographic (or image) data. Therefore, the flight planning problem shows different variants for different terrain types for both LiDAR data and simultaneous photographic data acquisition as test problems (mentioned in Table 1).

**Table 1: Problem Matrix with Problems Numbered from P1 to P4**

| Data Acquisition                           | Type of Terrain |                   |
|--|-----------------|-------------------|
|  | Flat Terrain    | Undulated Terrain |
| LiDAR data acquisition (alone)             | <b>P1</b>       | <b>P2</b>         |
| Simultaneous photographic data acquisition | <b>P3</b>       | <b>P4</b>         |

The number of constraints and consequently the complexities in flight planning problem increase from problem P1 to P4. Problems P1 and P4 consist of minimum and maximum number of constraints, respectively. In the following discussion, flight duration as fitness



The objective function, i.e., flight duration ( $T$ ), can be expressed as:

$$T = \frac{\sum_{i=1}^n L_i(\theta, X_i^L, X_i^R)}{V} + T_T \quad \dots (1)$$

where

$$\begin{bmatrix} X \\ Y \end{bmatrix} = \begin{bmatrix} \cos \theta & \sin \theta \\ -\sin \theta & \cos \theta \end{bmatrix} \begin{bmatrix} x \\ y \end{bmatrix} \quad \dots (2)$$

$$N = \left( \frac{Y_{\max} - Y_{\min}}{B} \right) \quad \dots (3)$$

$$n = \lceil N \rceil \quad \dots (4)$$

$\theta$  = Flying direction w.r.t.  $x$ -axis on map in counter-clockwise direction,

$X_i^L$  = Value of  $X$  coordinate of left edge (or left end) of  $i^{\text{th}}$  flight strip (or flight line) in rotated AOI,

$X_i^R$  = Value of  $X$  coordinate of right edge (or right end) of  $i^{\text{th}}$  flight strip (or flight line) in rotated AOI,

$L_i = |X_i^L - X_i^R|$  = Length of  $i^{\text{th}}$  flight strip (or flight line) from its start to end,

$Y_{\max}$  = Maximum value of  $Y$  coordinate (or ordinate) of rotated AOI,

$Y_{\min}$  = Minimum value of  $Y$  coordinate (or ordinate) of rotated AOI, and

$T_T$  = Total turning time computed using a procedure given in technical report on turning mechanisms [3]

Following constraints are considered for our problem. Generic constraints, which are common to all problems, (i.e. P1, P2, P3, and P4), are described first:

$$\rho \geq \rho_L \quad \dots (5)$$

$$\frac{|d_A - d_S|}{d_A} \leq \varepsilon_d \quad \dots (6)$$

$$(1000 - f \phi) \geq 0 \quad \dots (7)$$

$$\sigma_p \leq e_H \quad \dots (8)$$

$$\sigma_v \leq e_V \quad \dots (9)$$

$$H \geq h_{\max} + ESD \quad \dots (10)$$

$$H \geq h_{\max} + H_{\min} \quad \dots (11)$$

Additional constraints exclusive for problems P1 and P3:

$$\rho \leq \rho_U \quad \dots (12)$$

Additional constraints for problem P2 and P4:

$$\tau_\rho \leq \tau_{Max} \quad \dots (13)$$

Constraints for problems P3 and P4:

$$t_{ei} \leq \left( \frac{GSD(1 - P_{cx}) n_{px}}{V} \right) \quad \dots (14)$$

$$\phi_c \geq \phi_{opt} \quad \dots (15)$$

$$GSD \leq GSD_{Max} \quad \dots (16)$$

where

$$\rho = \left( \frac{F}{B_s V} \right), \quad \dots (17)$$

$$\sigma_p = \sqrt{\sigma_{X_p}^2 + \sigma_{Y_p}^2} \quad \dots (18)$$

$$\sigma_v = \sigma_{Z_p} \quad \dots (19)$$

$$P_R = dt/H \quad \dots (20)$$

$$\tau_\rho = P_R / (1 - P_R) \quad \dots (21)$$

$$B = (1 - P) B_s \quad \dots (22)$$

$$B_s = 2H \tan \phi \quad \dots (23)$$

$$P = 1 - (1 - P_R)(1 - P_{\min}) \quad \dots (24)$$

$$d_A = \left( \frac{V}{2f} \right) \quad \dots (25)$$

$$d_s = \frac{2f B_s}{F} \quad \dots (26)$$

$$GSD = \left( \frac{H s_p}{f_c} \right) \quad \dots (27)$$

$$\phi_{\max} \leq \tan^{-1} \left( K_{OC} \tan \left( \frac{\phi_{opt}}{2} \right) \right) \quad \dots (28)$$

$$K_{OC} = \left( \frac{1 - P_{ecy}}{1 - P_e} \right) \quad \dots (29)$$

$$P_{cx} = P_{ecx} + (1 - P_{ecx}) P_R \quad \dots (30)$$

Parameters of optimization problems are half scan angle ( $\phi$ ), scanning frequency ( $f$ ), flying height ( $H$ ), speed ( $V$ ), flying direction ( $\theta$ ), and PRF ( $F$ ). The ranges of these variables are presented in Table 2.

**Table 2: Working Ranges of Parameters of Optimization Problems**

| Parameter | Values   |                                    |
|-----------|--|------------------------------------|
|           | Range  | Least Count                        |
| $H$       | 80-3500 m  | Continuous                         |
| $\theta$  | 0-360°   | Continuous                         |
| $V$       | 45-72 m/s  | Continuous                         |
| $f$       | 1-70 Hz  | 1 Hz                               |
| $\phi$    | 1-25°  | 1°                                 |
| $F$       | {33, 50, 70, 100} kHz (if $80 \leq H \leq 1100$ m)<br>{33, 50, 70} kHz (if $1100 < H \leq 1700$ m)<br>{33, 50} kHz (if $1700 < H \leq 2500$ m)<br>{33} kHz (if $2500 < H \leq 3500$ m) | Discrete values depending upon $H$ |

Note that the half scan angle ( $\phi$ ) and scanning frequency ( $f$ ) are integer variables. Further, PRF ( $F$ ) is also a discrete variable, but depending on the values of the flying height ( $H$ ), it takes different values. The remaining variables in the problem are environmental constants presented in Table 3.

**Table 3: Values of Constants in Optimization Problem**

| Parameter       | Value                    |
|-----------------|--------------------------|
| $\rho_L$        | 10 points/m <sup>2</sup> |
| $\rho_U$        | 11 points/m <sup>2</sup> |
| $\tau_p$        | 30%                      |
| $\varepsilon_d$ | 10%                      |

|               |            |
|---------------|------------|
| $P_e$         | 10%        |
| $e_V$         | 0.10 m     |
| $e_H$         | 0.15 m     |
| $GSD_{Max}$   | 0.15 m     |
| $P_{ecx}$     | 60%        |
| $P_{ecy}$     | 25%        |
| $\beta_{max}$ | 25°        |
| $s_p$         | 0.000009 m |
| $n_{px}$      | 4092       |
| $f_c$         | 0.06 m     |
| $t_{ei}$      | 2.5 s      |

Mathematical expressions involved in the calculation of the total turning time are not shown here. The technical report [3] explains the procedure for calculating the total turning time. Similarly, calculations of  $\sigma_{X_p}, \sigma_{Y_p}, \sigma_{Z_p}$  are adopted from technical report [4]. Interested readers may obtain the details from these reports.

According to the problem formulation and also by the ranges and nature of the objective function and constraints, these are mathematically non-linear functions. In addition, the objective function is a discontinuous function. Moreover, the variables of optimization are integer, discrete and continuous variables, which are non-separable in the expressions of objective function and constraints. Furthermore, more specifically, as the number of options of values of PRF ( $F$ ) depends upon the range of the flying height ( $H$ ), it makes the problem a variable-size optimization problem. Therefore, for solving this optimization problem, use of genetic (or evolutionary) algorithm is inevitable.

### 3. Genetic Algorithm Essentials

Genetic algorithms (GAs) are flexible and versatile evolutionary optimization procedures that can be applied to problems having non-differentiability, discontinuity and mixed nature of variables. However, a GA is best applied if it is customized to solve a particular problem. In the following subsections, we describe the essential features that can be customized for an application and mention how they can be achieved for the flight planning problem described above.

### 3.1 Fitness Function for Handling Objective Function and Constraints

The fitness function in the selection operator is simply calculated by equation (1). Moreover, constraints are calculated using equations (5) to (16). Constraints are handled by the parameter less approach presented in [5].

### 3.2 Variable Handling

Variables in the design vector that are either integer, discrete, or their combination can be handled with GA. An integer variable, known with its upper and lower bound, is generated randomly by a bit string of predefined length. The value of the variable is obtained by decoding the bit string to decimal number. For example, the scanning frequency (with a range of 1-70 Hz) can be generated by decoding the 7 bit binary number which essentially results in integer numbers in the range of 0-127. The decoded decimal values beyond the relevant range of variables are rejected by additional inequality constraints. However, the GeneAS approach [6] advises to first generate all variables as real continuous numbers and then obtain the value of the integer variables by rounding the real number to the nearest integer. Moreover, PRF, which is a discrete variable, is also referred by lookup table. For this arrangement, as shown by equations (31) and (32), the continuous random number in range [0, 1] is mapped to discrete numbers of lookup table as each discrete number in lookup table refers to a value of discrete variable.

$$u_F = \begin{cases} u_F & 80 \leq H \leq 1100 \\ 0.75(u_F) & 1100 < H \leq 1700 \\ 0.5(u_F) & 1700 < H \leq 2500 \\ 0.25(u_F) & 2500 < H \leq 3500 \end{cases} \quad \dots (31)$$

$$F = \begin{cases} 33 \text{ kHz} & 0.00 \leq u_F \leq 0.25 \\ 50 \text{ kHz} & 0.25 < u_F \leq 0.50 \\ 70 \text{ kHz} & 0.50 < u_F \leq 0.75 \\ 100 \text{ kHz} & 0.75 < u_F \leq 1.00 \end{cases} \quad \dots (32)$$

In the forthcoming discussions, these two options of variable handling are abbreviated as MCV (mixed or binary plus real-coded variables) and RCV (real-coded variables).

### 3.3 Sampling of Initial Population

A population of design vector is generated by ordinary random sampling (ORS) method. However, instead of ORS, Latin hypercube sampling (LHS), which is a space filling sampling technique, should also be employed and tested for real world problems [7]. LHS generates the multivariate samples by random pairing of variables that exhibit the space filling property and multivariate uniformity [8]. The original LHS method, of McKay et al. [9], mentioned by Hess et al. [10] is adopted.

GA generates the values of a real parameter (say  $V$ ) between its given lower and upper bounds using a random number. The  $k^{th}$  sample or candidate of a population for a parameter  $V$ , which is calculated using a random number ( $r_k$ ) in range  $[0, 1]$ , can be written as:

$$V_k = (1 - r_k) V_{\min} + r_k V_{\max} \quad \dots (33)$$

For ordinary random sampling (ORS), the random number is a uniformly distributed random number. Therefore,

$$r_k = u_k \quad \dots (34)$$

However, for LHS, a random number  $r_k$  is calculated by generating the non-repeating random sequence of numbers 1 to  $m$  numbers as [11]-[12]:

$$r_k = \left( \frac{\pi_k - u_k}{m} \right) \quad \dots (35)$$

Where

$V_{\min}$  = Lower bound of variable  $V$

$V_{\max}$  = Upper bound of variable  $V$

$r_k$  = Random number for generating a random value of variable  $V$

$m$  = Population size (number of samples)

$u_k$  = Uniformly distributed random number in range  $[0, 1]$

$\pi_k = k^{th}$  member of non-repeating sequence

Random number ( $\pi_k$ ) in non-repeating sequence and uniformly distributed random number ( $u_k$ ) should be generated independently. The random permutations for each variable ensure the random pairing of variables in multi-dimension [13].

The random non-repeating sequence of samples of a particular variable can be generated by random permutation algorithm [14]. The random permutation algorithm shuffles a sequence of  $m$  numbers randomly in an unbiased manner. Independently shuffled sequences of  $m$  numbers for each variable individually generate random pairs of variables with multivariate uniformity and space filling property [13].

### 3.4 Elite Preservation

For a particular generation, a design vector (or a candidate in a given population) which provides THE optimal value (minimum value for a minimization problem) is named as ‘current best’. However, the mechanism of elitism prefers to preserve the candidate that brings the optimal fitness function over the generations. The preserved candidate is called the ‘best ever’. After a particular generation, if the ‘best ever’ is found to be inferior to the ‘current best’, the value stored in the ‘best ever’ is updated by the value of the ‘current best’. According to the elitism, the ‘best ever’ unconditionally participates in next generation by replacing another candidate in a population. Induction of elitism avoids the straying of the evaluation process towards a sub-optimal solution and thus enhances the probability of detection of global optimal solution. However, on the other hand, the elitism principle reduces the diversity of population over generations and thereby it is also suspected of early or premature convergence.

Replacement of a candidate in population by the ‘best ever’ is performed with different strategies. In this paper, including the elite-less evaluation, the following four methodologies are used for elitism.

(a) **No elites (NE):** Elitism is not adopted and the ‘best ever’ is neither evaluated nor recorded. In other words, only the ‘current best’ is evaluated in a generation for reporting

purpose. ‘Current best’ can not affect the next generation directly as its unconditional participation in the next generation is not allowed.

(b) **‘Best ever’ replaces the current worst (BRCW):** Contrary to the ‘current best’, the ‘current worst’ is defined as a candidate that provides the worst value of fitness function (maximum value for a minimization problem) in a generation. The ‘current worst’ is replaced by the ‘best ever’ [15].

(c) **‘Best ever’ replaces a candidate by niching (BRCN):** The ‘best ever’ replaces a candidate which is most similar to the ‘best ever’ itself. This process is also known as the objective space *niching* (OSN). For evaluating the most similar candidate, first a specific percentage (say 20%) of population is chosen randomly from the population. Among the chosen candidates, the most similar candidate has minimum Euclidean distance in parameter space from the ‘best ever’. The percentages of chosen candidates may vary from 0 to 100%. However, 0% arrangement resembles to ‘No elites (NE)’ and increasing percentage of chosen candidates will raise the computation cost considerably.

(d) **‘Best ever’ replaces a candidate randomly (BRCR):** The ‘best ever’ replaces a candidate which is chosen randomly from a population [15].

### **3.5 Parameter Space Niching**

The discussion so far considers the possibility of multiple local optima while assuming prominent and dominating global optima compared to local ones. However, during the evaluation process by GA, it is possible that in a certain generation, the majority of population members are attracted towards a local optimum and very few are attracted towards a global optimum. Consequently, due to the higher number of population members being attracted towards the local optimum, the GA will be biased towards the local optima in the subsequent generations. It generally happens for competing optima which are spread across the parameter space that the majority of the population candidates may be attracted towards a local optimum. As a result, the evaluation process of GA may get trapped around a local optimum. Due to this bias, a global optimum that is

located by a smaller number of candidates is apparently ignored. Therefore, in a multi-modal problem, even the ‘best ever’ evaluated over many generations may possibly be a local optimum which may be an inferior result.

The problem of trapping of the GA solution in a local optimum for a multi-modal optimization problem is resolved by parameter space *niching* [16]. The parameter-space *niching* considers objective or fitness values of candidates, which are available in the vicinity of a local optimum. According to the expected number of optima in a parameter space, Deb [17] suggests to assume the parameter space divided amongst the optima and considers a hyper-sphere around an optimum. Degrading the fitness values of all candidates falling around a local optimum within the hyper-sphere by a predefined factor gives an opportunity to other candidates to play a significant role in the subsequent generations. The following formula is mentioned to calculate the value of *niching* radius of hyper sphere ( $\sigma_{share}$ ) in normalized parameter space [17] (on page 155):

$$\sigma_{share} = \left( \frac{0.5}{(q)^{1/p}} \right) \quad \dots (36)$$

where

$p$  = Number of parameters in optimization problem

$q$  = Number of expected optima in complete parameter space

In order to implement parameter space *niching*, Deb [17] recommends to use  $q$  in the range of 5-10 for the real-world problems. However, our purpose of using parameter space *niching* is to preserve the diversity in the population so that few solutions, which are found in the global basin of attraction do not get ignored, we assume that the problem has  $q=10$  optima and accordingly we choose  $\sigma_{share}$  equals to 0.340646 in this study.

The next section discusses the proposed configuration of a GA using the above strategies and the subsequent section implements the derived algorithm for solving the flight planning problem for airborne LiDAR data acquisition.

#### 4. Proposed GA

The discussed options for configuration of GA create several combinations of algorithms as mentioned strategies are independent and thus can be implemented individually. The following table consolidates all discussed options (or strategies) suggested.

**Table 4: Configuration Parameters of RGA Code**

| S.N. | Strategy (number of options)              | Details (abbreviated names) of options |
|------|---|--|
| 1.   | Variable handling (2)                     | BCV, RCV                               |
| 2.   | Sampling (2)                              | ORS, LHS                               |
| 3.   | Elitism (4)                               | NE, BRWC, BRCN, BRGR                   |
| 4.   | Parameter space <i>niching</i> or PSN (2) | PSN or Without PSN                     |

The options in the above table suggest 32 permutations which can be tested on any real-world problem. In view of various algorithms, it is required to investigate the possible configurations of GA and determine a configuration that can be universally accepted for an optimization problem. In order to implement these algorithms, the Real-Coded Genetic Algorithms (RGA) code and Non-dominated Sorting Genetic Algorithms-II (NSGA-II) code [18], which are available online from KanGAL's website (<http://www.iitk.ac.in/kangal/codes.shtml>) for solving the single objective and multi-objective optimization problems, respectively, are used in this study.

The RGA and NSGA-II codes that respectively optimize the single and multi-objective optimization problems with normalized constraints, handle continuous and discrete variables as real and binary coded design variables, respectively. All the details regarding the initialization of population, selection process, crossover, mutation and constraint handling strategies are commented in the available codes. The population is generated in the initialization process by ordinary random sampling (ORS) method, as discussed in Section 3.3. The selection is performed by the tournament selection method. The available code uses the single point crossover [1] and simulated binary crossover (or SBX) [19] for binary and real variables, respectively. The bit-wise mutation is carried out for the binary coded GA while the polynomial mutation [20] is used for the real coded GA. The constraints are handled using the Deb's parameter-less approach [5]. For a multi-modal problem, the code also has a provision for parameter space *niching* [17] which is already discussed in detail in the previous section. The codes also provide a file

output with solution of design vector and values of fitness function and constraints. Specific details about the RGA code and NSGA-II code are explicitly mentioned in Deb [21] and Deb et al. [18], respectively.

The resulting combinations of test problems (P1 to P4) and 32 different algorithms, described in previous sections, result in a large number of options to be evaluated. Thus we desire a deductive approach in which 10 algorithms (A1-A10) are considered with 4 problems (P1 to P4). The purpose of testing multiple algorithms, whose genesis is discussed in the above section, is to identify a set of algorithms that show the best performance on the test problems. According to the performance, appropriate algorithms can be identified and prioritized. As a result, the available default RGA code, as algorithm A1, is utilized at first and based on its performance new algorithms are derived. The forthcoming discussion details the results of single objective constrained minimization of test problems. Moreover, next section also describes a diligent approach of implementing the GA algorithms to solve a minimization problem.

## **5. Results of Single Objective Optimization**

The following discussion designs a set of algorithms with the default RGA code as the first or base algorithm. The simulations are performed on computer machines having ‘Intel Core 2 Q9550 Quad processors (2.83 GHz)’ and ‘Intel Core i3 530 processors (2.93 GHz)’. The statistical measures (minimum, maximum, average and standard deviation) of flight duration are evaluated for 30 runs of each algorithm. Moreover, number of outliers is also detected manually. Lower value of standard deviation and less number of outliers show the convergence and consistency, respectively, in the results obtained by the algorithm.

The default RGA code facilitates the use of binary coded integer and real coded continuous variables with ORS and no elite preservation. As the half scan angle ( $\phi$ ) and scan frequency ( $f$ ) are integer variables, the mixed variable approach (combination of integer and continuous variables) is used. In order to decide the better variable handling strategy, the default algorithm with mixed variables (binary coded discrete variables and

real coded continuous variables) and a population count equal to 60 are first employed with four elite preservation strategies against the first test problem P1. None of the four algorithms perform as desired and thus results are not presented here. Further increasing the population count to 200, which is more than 3 times the recommended value, also do not find an acceptable solution. The probable reason is that GA is restricted to explore the discrete variables amongst the integer numbers with standard indices of crossover and mutation operators, as exploring and regenerating in the limited integer numbers cannot reach to a specific value. However, as has been discussed earlier, all variables including integer ones, can also be treated as real coded variables [6]. When integer variables are coded as rounded real variables, the first three algorithms (A1, A2, A3) can find feasible results for problem P1 with a population count of 60. A result generated by RGA code is declared outlier if the optimum value of the flight duration is not similar to the majority of the flight duration values for other runs. Increasing the population to 120 and 200 reduced both the number of outliers and the standard deviation of the flight duration. However, algorithm A4 cannot find any feasible result with any population count (60, 120, and 200). On the other hand, the solutions determined by the algorithm A2 are feasible, though all solutions appeared as outliers when compared with the results of A1 and A3. The results are tabulated below with the details of the algorithms. Table 5 below also indicates the number of outliers and feasible results.

**Table 5: Statistical Results of Simulation of Test Problem P1 with Algorithms A1 to A3**

| <b>Problem P1: LiDAR Data Acquisition Alone on Flat Terrain</b> |                              |                              |                              |  |   |
|---|------------------------------|------------------------------|------------------------------|--|---|
| <b>Algorithm</b>  | <b>Minimum<br/>(seconds)</b> | <b>Maximum<br/>(seconds)</b> | <b>Average<br/>(seconds)</b> | <b>Standard<br/>Dev.<br/>(seconds)</b> | <b>Outliers/<br/>Feasible<br/>Results</b> |
| <b>Population = 60</b>  |                              |                              |                              |  |   |
| A1<br>(RCV+ORS+NE )   | 1572.888                     | 1598.427                     | 1580.223                     | 7.828                                  | 11/30                                     |
| A2<br>(RCV+ORS+BCRW)  | 1820.020                     | 1841.703                     | 1822.215                     | 5.303                                  | 0/30                                      |
| A3<br>(RCV+ORS+BRCR)  | 1572.513                     | 1603.716                     | 1576.998                     | 7.4                                    | 11/30                                     |
| <b>Population = 120</b>   |                              |                              |                              |  |   |
| A1<br>(RCV+ORS+NE )   | 1572.557                     | 1652.099                     | 1585.951                     | 21.784                                 | 5/30                                      |
| A2<br>(RCV+ORS+BCRW)  | 1573.154                     | 1635.079                     | 1585.295                     | 18.442                                 | 6/30                                      |
| A3<br>(RCV+ORS+BRCR)  | 1572.552                     | 1583.484                     | 1575.007                     | 30.037                                 | 4/30                                      |
| <b>Population = 200</b>   |                              |                              |                              |  |   |

|                      |          |          |          |        |      |
|----------------------|----------|----------|----------|--------|------|
| A1<br>(RCV+ORS+NE )  | 1572.77  | 1655.552 | 1585.177 | 19.83  | 5/30 |
| A2<br>(RCV+ORS+BCRW) | 1573.152 | 1655.552 | 1584.701 | 18.341 | 4/30 |
| A3<br>(RCV+ORS+BRCR) | 1572.749 | 1587.435 | 1573.854 | 2.739  | 2/30 |

The analysis of performance of the algorithms A1 to A4 for test problem P1 indicates that three strategies demonstrate the capability of optimization. For algorithm A2, for the population count of 60, none of the results are outliers but the obtained fitness value is worse than that of other algorithms. This may be due to the premature convergence, which generally happens if the population can not explore the complete parameter space and consequently reaches to inferior optimum. However, for population count of 120 and 200, the effect of the premature convergence reduces. On the other hand, the fourth strategy (algorithm A4) can not find any feasible solution in all 30 runs. The probable reason is difficult to quote without attempting this algorithm for other problems.

With the performance shown above, the simulations are performed for the test problem P2 with all four algorithms. All four algorithms are able to resolve the problem of minimization for problem P2. However, the number of outliers for the population counts of 60 and 120 for over 30 runs are in the range of 9-15. Therefore, the results for the population count of 200 only are shown in Table 6.

**Table 6: Statistical Results of Simulation of Test Problem P2 with Algorithms A1 to A4**

| <b>Problem P2: LiDAR Data Acquisition Alone on Undulated Terrain<br/>Population = 200</b> |                              |                              |                              |  |   |
|---|------------------------------|------------------------------|------------------------------|--|---|
| <b>Algorithm</b>  | <b>Minimum<br/>(seconds)</b> | <b>Maximum<br/>(seconds)</b> | <b>Average<br/>(seconds)</b> | <b>Standard<br/>Dev.<br/>(seconds)</b> | <b>Outliers/<br/>Feasible<br/>Results</b> |
| A1<br>(RCV+ORS+NE )   | 1874.318                     | 1994.195                     | 1918.523                     | 40.679                                 | 6/30                                      |
| A2<br>(RCV+ORS+BCRW)  | 1874.318                     | 1994.195                     | 1918.523                     | 40.678                                 | 6/30                                      |
| A3<br>(RCV+ORS+BRCR)  | 1864.442                     | 1902.133                     | 1873..662                    | 7.656                                  | 3/30                                      |
| A4<br>(RCV+ORS+BRCN)  | 1863.670                     | 1903.895                     | 1872.565                     | 8.153                                  | 3/30                                      |

As shown in Table 6, algorithms A3 and A4 performed considerably well when compared to algorithm A1 and A2 against the criteria of standard deviation and number

of outliers. Algorithms A1 and A2 show low consistency figures (higher number of outliers) and higher standard deviation values. The low consistency may be due to the multiple optima being located very close to each other and GA is occasionally detecting any one of them. Moreover, as stated earlier, if inferior optima appear in large numbers, these may be detected as optima with a higher probability. Considering this possibility of multiple local optimums, parameter space *niching* is deployed and the algorithms A1 and A2 are upgraded. However, no significant improvement is observed even with this modification. On the other hand, in anticipation of further improvement in the performance, algorithms A3 and A4 are upgraded to the algorithms A5 and A6 by adopting the parameter space *niching*. The *niching* radius, expressed by equation (36), is calculated for an anticipated number of multi-optimums (i.e., equal to 10). Once again, no significant improvement is observed in the minimum value of the objective function and in the consistency of results. Moreover, algorithm A6, which is an up-gradation of the algorithm A4, show slight degradation in the results compared to results of A4. On the other hand, parameter space *niching* is successful in reducing the magnitudes of outliers.

**Table 7: Statistical Results of Simulation of Test Problem P2 with Algorithms A5 to A6**

| <b>Problem P2: LiDAR Data Acquisition Alone on Undulated Terrain</b> |                              |                              |                              |  |   |
|--|------------------------------|------------------------------|------------------------------|--|---|
| <b>Population= 200, Niching Radius = 0.340646;</b>                   |                              |                              |                              |  |   |
| <b>Algorithm</b>   | <b>Minimum<br/>(seconds)</b> | <b>Maximum<br/>(seconds)</b> | <b>Average<br/>(seconds)</b> | <b>Standard<br/>Dev.<br/>(seconds)</b> | <b>Outliers/<br/>Feasible<br/>Results</b> |
| A5<br>(RCV+ORS+BRCR+PSN)   | 1865.403                     | 1902.398                     | 1874.327                     | 9.593                                  | 3/30                                      |
| A6<br>(RCV+ORS+BRCN+PSN)   | 1865.180                     | 1952.882                     | 1879.162                     | 19.275                                 | 5/30                                      |

A critical observation of the minimum values of the fitness function (Tables 6 and 7), obtained by the algorithms A3, A4, A5 and A6, indicates that each algorithm obtains similar values of the minimum flight duration at least once over 30 runs. Therefore, a more detail analysis of the chosen algorithms is required to investigate what features of the algorithms are important.

The standard deviation values are shown in Tables 6 and 7, which suggest that GA is severely affected by bias. The anticipated bias, which may be developed in GA implementation at any stage, from its initialization to the end of last generation, is

generally overcome by increasing the mutation probability or population count. Increasing the mutation probability in algorithm A5 and A6 degrades the results. However, increasing the population count to 200 or higher reduces the standard deviation of fitness values. A higher number of samples generated with increased population count perhaps explored the parameter space more rigorously and therefore, it further indicates that bias is inducted by the sampling method. Consequently, the sampling by LHS is adopted for initialization of the population. The upgraded algorithms are A7, A8, A9 and A10. Algorithms A7 and A8 utilize the LHS alone whereas additionally the parameter space *niching* is also applied in algorithms A9 and A10. As sampling method of GA is changed, the simulations for all four algorithms (A7, A8, A9 and A10) are attempted for population count of 60, 120 and 200. However, for a population count of 60 and 120, the numbers of outliers are in the range of 5-8 for A7 and 5-17 for A8, respectively. Additionally, with the same population count of 60 and 120 for algorithms A9 and A10, the number of outliers is slightly less. However, for population count of 200, all four algorithms perform almost in similar manner as there are no major differences in the values of outliers or standard deviations. Results of population count 200 are presented in Tables 8 and 9.

**Table 8: Statistical Results of Simulation of Test Problem P2 with Algorithms A7 to A8**

| <b>Problem P2: LiDAR Data Acquisition Alone on Undulated Terrain<br/>Population = 200</b> |                              |                              |                              |  |   |
|---|------------------------------|------------------------------|------------------------------|--|---|
| <b>Algorithm</b>  | <b>Minimum<br/>(seconds)</b> | <b>Maximum<br/>(seconds)</b> | <b>Average<br/>(seconds)</b> | <b>Standard<br/>Dev.<br/>(seconds)</b> | <b>Outliers/<br/>Feasible<br/>Results</b> |
| A7<br>(RCV+LHS+BRCR)  | 1865.051                     | 1880.460                     | 1873.351                     | 5.427                                  | 4/30                                      |
| A8<br>(RCV+LHS+BRCN)  | 1865.251                     | 1902.768                     | 1872.735                     | 8.619                                  | 5/30                                      |

**Table 9: Statistical Results of Simulation of Test Problem P2 with Algorithms A9 to A10**

| <b>Problem P2: LiDAR Data Acquisition Alone on Undulated Terrain<br/>Population = 200; Niching Radius = 0.340646</b> |                              |                              |                              |  |   |
|--|------------------------------|------------------------------|------------------------------|--|---|
| <b>Algorithm</b>   | <b>Minimum<br/>(seconds)</b> | <b>Maximum<br/>(seconds)</b> | <b>Average<br/>(seconds)</b> | <b>Standard<br/>Dev.<br/>(seconds)</b> | <b>Outliers/<br/>Feasible<br/>Results</b> |
| A9<br>(RCV+LHS+BRCR+PSN)   | 1865.066                     | 1882.392                     | 1874.327                     | 5.047                                  | 4/30                                      |
| A10<br>(RCV+LHS+BRCN+PSN)  | 1864.308                     | 1886.427                     | 1871.788                     | 6.188                                  | 4/30                                      |

As is evident from the results presented in Table 9, an insignificant improvement is observed due to the parameter space *niching*. Consequently, due to the extra computational load in comparison to the gain in the result by the parameter space *niching*, the algorithms A9 and A10 are discarded. As a result, the algorithms A7 and A8 are applied on the test problems P3 and P4. The results are shown in Tables 10 and 11.

**Table 10: Statistical Results of Simulation of Test Problem P3 with Algorithms A7 to A8**

| <b>Problem P3: LiDAR and Photographic Data Acquisition on Flat Terrain</b> |                              |                              |                              |  |   |
|--|------------------------------|------------------------------|------------------------------|--|---|
| <b>Population = 200</b>  |                              |                              |                              |  |   |
| <b>Algorithm</b>   | <b>Minimum<br/>(seconds)</b> | <b>Maximum<br/>(seconds)</b> | <b>Average<br/>(seconds)</b> | <b>Standard<br/>Dev.<br/>(seconds)</b> | <b>Outliers/<br/>Feasible<br/>Results</b> |
| A7<br>(RCV+LHS+BR CR)  | 1572.604                     | 1576.200                     | 1573.309                     | 0.748                                  | 1/30                                      |
| A8<br>(RCV+LHS+BR CN)  | 1572.560                     | 1577.897                     | 1573.531                     | 1.109                                  | 0/30                                      |

**Table 11: Statistical Results of Simulation of Test Problem P4 with Algorithms A7 to A8**

| <b>Problem P4: LiDAR and Photographic Data Acquisition on Undulated Terrain</b> |                              |                              |                              |  |   |
|---|------------------------------|------------------------------|------------------------------|--|---|
| <b>Population=200</b>   |                              |                              |                              |  |   |
| <b>Algorithm</b>  | <b>Minimum<br/>(seconds)</b> | <b>Maximum<br/>(seconds)</b> | <b>Average<br/>(seconds)</b> | <b>Standard<br/>Dev.<br/>(seconds)</b> | <b>Outliers/<br/>Feasible<br/>Results</b> |
| A7<br>(RCV+LHS+BR CR)   | 1941.770                     | 1948.097                     | 1944.136                     | 1.804                                  | 1/30                                      |
| A8<br>(RCV+LHS+BR CN)   | 1942.317                     | 1949.325                     | 1944.609                     | 2.069                                  | 0/30                                      |

### 5.1 Selection of the Best Algorithm

Apart from the observations on performance and analysis of algorithms for various problems (P1 to P4), selection of algorithm is equally important. An algorithm that show minimum number of outliers (consistency) and determines the flight duration with minimum variation (convergence) is better than other algorithms.

As shown previously that for problems P2, P3, and P4, standard deviations of the flight duration values over 30 runs by algorithms A7 and A8 are considerably less compared to the other algorithms. Moreover, a pattern of reduction in the numbers of outliers, when population increases, is also observed. As a result, it can be inferred that algorithms A7 and A8 are able to solve the minimization problem with maximum number of constraints (i.e. problem P4). However, considering the additional calculations in algorithm A8, due

to the objective space *niching*, the algorithm A7 appears a good trade off in performance and speed. There is a possibility of achieving better performance of algorithm A8 by increasing the fraction of population considered for evaluating the most similar candidate for the ‘best ever’. However, due to the smaller standard deviation observed in the fitness values and flight planning parameter values, and less computational load in decision making process, the algorithm A7 can be accepted as a better algorithm without hesitation.

## **6. Results of Multi-Objective Optimization**

As indicated earlier, when a user wants to understand the variation of flight duration or trade-off against the constraints, the single-objective minimization approach sometimes cannot suffice the purpose. An alternative approach considers the potential of multi-objective optimization, which allows integration of two or more conflicting objectives in a single framework. The multi-objective optimization is performed by the NSGA-II code here. The error in LiDAR data has an inverse relationship with the flight duration, as improving the former decreases the latter [2]. As both planimetric and altimetric errors increase with the decrease in flight duration, the 3D error minimization is considered as the second objective in the NSGA-II code. Alike 3D errors, the effective swath ( $B$ ) is also conflicting with the flight duration. However, flight planners are generally not interested to know about the trade-off between effective swath and flight duration. Therefore, in this paper, authors show the compromise solutions of flight duration with altimetric and planimetric errors in detail.

### **6.1 Bi-objective Optimization by NSGA-II Code**

With LHS method and RCV for parameters, simulations are run by NSGA-II code for 300 generations and a population count of 2,000. The results showing trade-off between the two conflicting objectives are obtained by NSGA-II code with the flight duration being the first objective (on  $y$ -axis) and one of the altimetric error or planimetric error being as the second objective (on  $x$ -axis).

The problems P1 to P4 involve all the mentioned variables (i.e., planimetric error, altimetric error), though the multi-objective optimization by NSGA-II code is performed only for problems P2 and P4 as both contain the maximum number of constraints for simultaneous LiDAR and photographic data acquisition. When the problems, P2 or P4, are solved as a single-objective constrained minimization problem, the original planimetric and altimetric errors are treated as constraints representing the minimal requirement of desired data. In multi-objective optimization, in addition to be used as constraints, one of altimetric or planimetric error is also considered as second objective in NSGA-II code. The fronts of optimal values showing the compromising results for two variables against the flight duration are plotted as shown in Figures 3 to 6. We discuss these plots in the following paragraph.

The NSGA-II code plots the values of flight duration for all values of the vertical and horizontal errors ( $1\sigma$ ) which are less than 10 cm and 15 cm, respectively, as the vertical and horizontal errors are restricted up to these values. Moreover in all plots, the zones with no points indicate gaps (mainly due to the absence of any feasible solution in these regions, which we demonstrate in the next paragraph) in the obtained front. Figures 3 to 4 and Figures 5 to 6 are drawn for problems P2 and P4, respectively. For problem P4, in comparison to problem P2, due to higher number of constraints, the feasible zones are smaller for all variables (second objective) as is evident from the comparison of figures.

Before making any inference using these plots, it should be first confirmed whether the front containing compromise solutions are truly Pareto-optimal. A Pareto-optimal front contains trade-off solutions that cannot be improved for both objectives simultaneously. Although mathematical optimality conditions involving derivatives of objectives and constraints and certain regularity conditions are needed to prove Pareto-optimality of every point, here we make an attempt to build confidence about their optimality by solving several single-objective epsilon-constraint (EC) problems. EC method, which is briefly explained by Mavrotas [22], minimizes the first objective as a single-objective problem with an additional constraint on the second objective that is conflicting with the first one. For example, the flight duration is minimized by the RGA code with a

constraint that planimetric error should be less than or equal to 13.6 cm (for example) in Figure 3. If a Pareto-optimal solution exists between the gap (having planimetric error within 13.1cm and 14.3cm), the above epsilon-constraint optimization problem should find it. This would then validate the gap indicated by the NSGA-II solutions. In the figure, points obtained by NSGA-II showing the trade-off between the FD and planimetric errors are connected by firm lines to show the non-dominated region in the upper half of the figure. Constraints on FD and errors are shown by horizontal and vertical dashed lines, respectively.

EC method is deployed with 2,000 population members and is run for 300 generations with algorithm A7. Solutions are obtained by minimizing the flight duration under the original constraints of altimetric and planimetric errors and with the above additional constraint (planimetric error is less than or equal to 13.6 cm (marked as constraint 2 in Figure 3)). Interestingly, the obtained solution does not lie within the gap, instead it lies close to the planimetric error of 13.1 (marked as '2' in the figure 3) – a solution also obtained by NSGA-II. This indicates that a feasible solution does not exist within the gap and this is the reason NSGA-II found a fragmented set of trade-off solutions. One other epsilon-constraint formulation is performed with an additional planimetric error limited to 13.2 cm (constraint marked as 1 in Figure 3) and the obtained solution is close to one of the NSGA-II solution (marked as '1'). Constraints on flight duration at two different values (2,200 and 2,500 sec) are tried next and planimetric error objective is minimized. Corresponding optimized solutions are marked as 'a' and 'b', respectively. All these independent single-objective minimizations amply indicate that there does not lie any feasible solution in the gaps present in the fragmented NSGA-II front.

To further validate the extreme solutions, we perform independent minimization of each objective with the original constraints alone. The optimized solutions are marked with a star (FD minimization) and with a 'x' (PE minimization). The optimized solutions are slightly worse than the respective extreme NSGA-II solutions. The presence of gaps certainly makes the search process difficult and this study demonstrates the efficacy of the suggested NSGA-II approach for solving the flight planning optimization problem.

Similar studies of epsilon-constraint minimization to validate observed gaps in NSGA-II fronts and individual objective minimization to validate the extreme NSGA-II solutions are performed for other three bi-objective optimization problems in Figures 4, 5 and 6.

Table 12 displays extreme values of FD and altimetric error, and the salient points obtained by EC method by constraining the FD and altimetric error for problem P4.

**Table 12: Extreme Values and Results of EC Method for Problem P4**

| <b>Constraint</b>   | <b>Flight Duration (FD) (seconds)</b> | <b>Altimetric Error (AE) (cm)</b> | <b>Constrained Marked by</b> | <b>Solution Marked by</b> |
|---|---------------------------------------|-----------------------------------|------------------------------|---------------------------|
| <b>Minimizing the Altimetric Error (AE) with Constrained Flight Duration (FD)</b>       |                                       |                                   |                              |                           |
| FD ≤ 2100 seconds   | 2090.80                               | 8.0612                            | Line A                       | Point a                   |
| FD ≤ 2800 seconds   | 2799.66                               | 8.0373                            | Line B                       | Point b                   |
| FD ≤ 4500 seconds   | 2837.46                               | 8.0373                            | Line C                       | Point c                   |
| <b>Minimizing the Flight Duration (FD) with Constrained Altimetric Error (AE)</b>       |                                       |                                   |                              |                           |
| AE ≤ 8.03 cm  | 3899.01                               | 8.0241                            | Line 1                       | Point 1                   |
| AE ≤ 8.04 cm  | 2727.41                               | 8.0385                            | Line 2                       | Point 2                   |
| AE ≤ 8.06 cm  | 2727.32                               | 8.0385                            | Line 3                       | Point 3                   |
| <b>Extreme Values: Minimum Values of Flight Duration (FD) and Altimetric Error (AE)</b> |                                       |                                   |                              |                           |
| Minimizing FD   | <b>1931.94</b>                        | 8.0729                            |                              | <b>Star (*)</b>           |
| Minimizing AE   | 5334.03                               | <b>8.0239</b>                     |                              | <b>Cross (x)</b>          |

As indicated in Table 12, the values obtained by EC method are marked in Figure 6 by alphabets **a**, **b**, **c** and numbers **1**, **2**, **3**. Interestingly, as evident from the Table 12, point 2 and 3, and **b** and **c** are clustered.

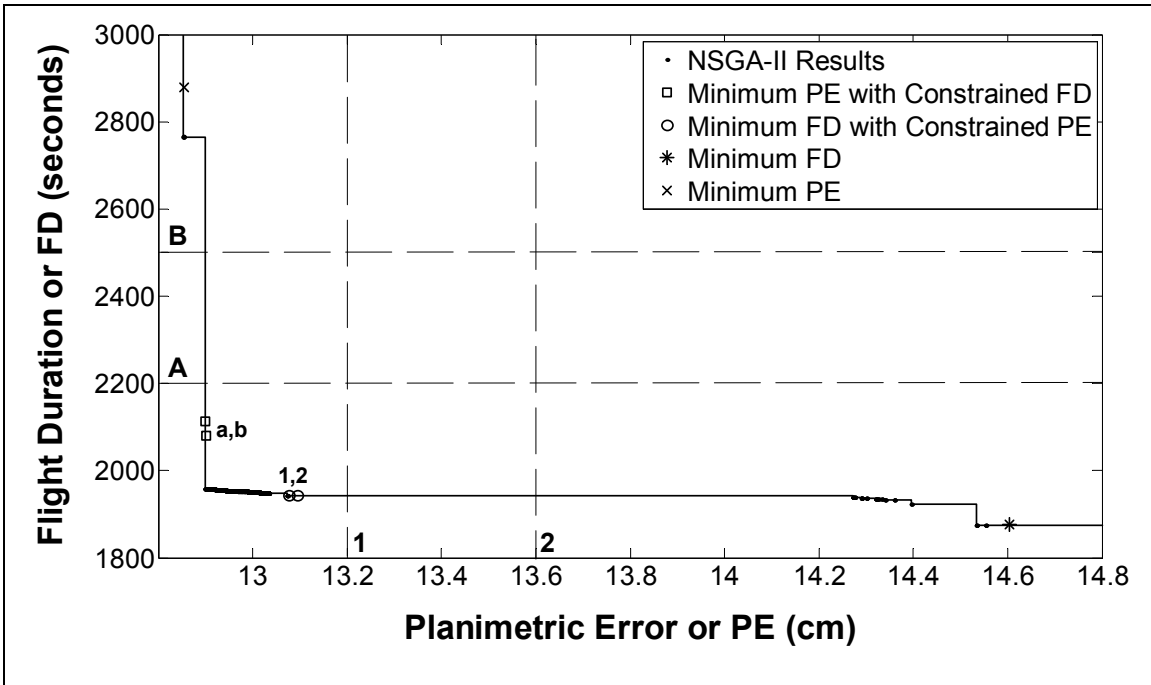


Fig. 3: Pareto-optimal front (flight duration v/s planimetric error) for P2. A, B and 1, 2 constraints are discussed in the text.

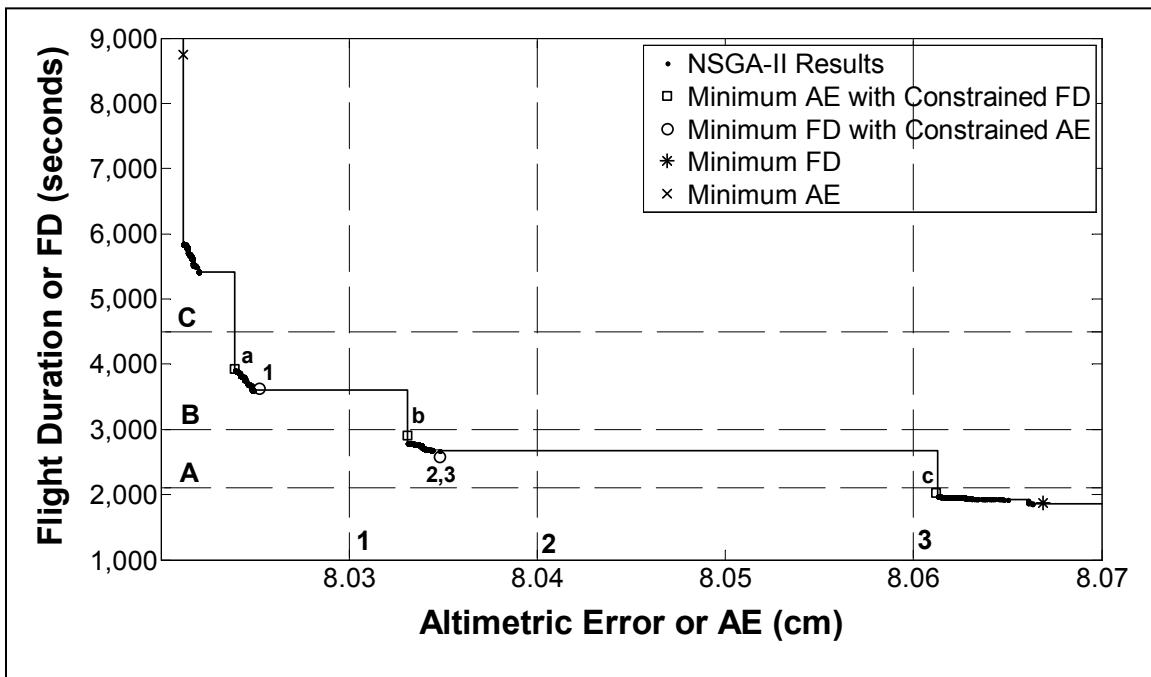


Fig. 4: Pareto-optimal front (flight duration v/s altimetric error) for P2

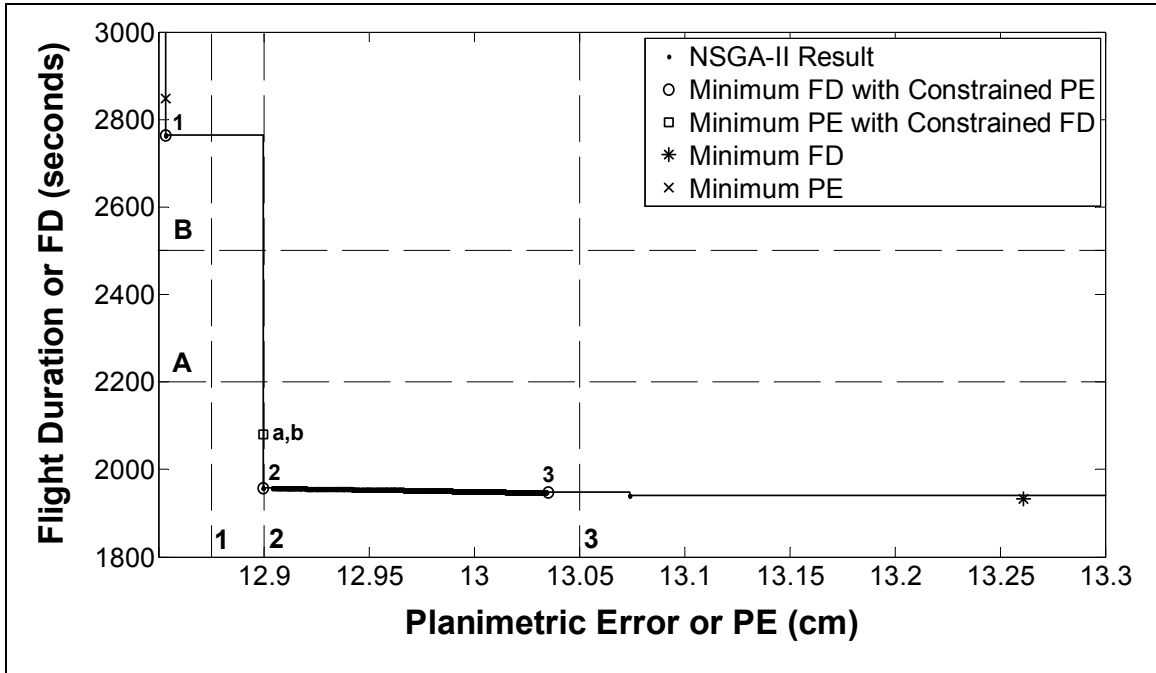


Fig. 5: Pareto-optimal front (flight duration v/s planimetric error) for P4

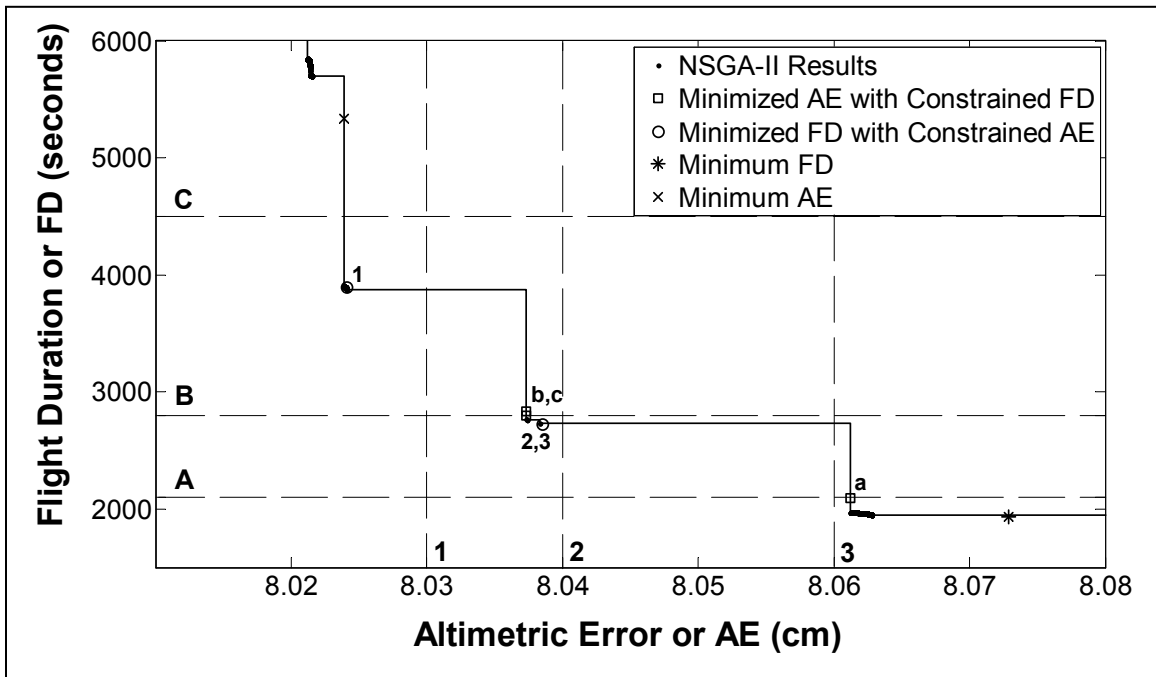


Fig. 6: Pareto-optimal front (flight duration v/s altimetric error) for P4

Having obtained confidence in the NSGA-II front, the next section presents a general analysis and interpretation of these results as well as the physical significance of these results for the flight planning problem.

## **6.2 Analysis, Interpretation, and Physical Significance of Multi-Objective Results:**

NSGA-II plots are useful in three ways:

- (i) Plots shown by Figures 3 to 6 shows that almost all points, which are lying on the Pareto-optimal front, are detected by NSGA-II, except the extreme minimum values of two conflicting objectives. In most of the cases, extreme points are lying outside the range of Pareto-optimal front. However, in some of the cases, for example in Figures 4 and 6, NSGA-II cannot detect the optima which are indicated by single-objective minimization. These results (by single-objective minimization) clearly suggest that if the desired solution lies in a particular region(s) of the Pareto-optimal front, these regions should be thoroughly explored by single objective problem under region specific constraints.
- (ii) When the second objective, which is also a constraint, is restricted between lower and upper bounds, these plots convey important information about the required FD and corresponding values of the flight planning parameters. For example, the maximum value of vertical error ( $1\sigma$ ) is 10 cm. However, a flight planner may want to know the FD information for the vertical error that is in the range of 7-9 cm. Though it can be obtained by single objective optimization, limiting the vertical error by lower and upper bounds in the single objective optimization will add one more constraint and reduces the feasible parameter space for determination of the unique solution. A smaller feasible parameter space imposes an increased complexity in the problem which therefore demands higher population count and thus raising the need of higher computational time. However, the multi-objective optimization exhibits the variation between the flight duration and the vertical error, which are conflicting objectives, in the form of non-dominated front. Therefore, using these plots of Pareto-optimal front, a flight planner can also change the flight plan for achieving a better accuracy (or less errors) than 10 cm in vertical direction

with the information about the respective increase in the flight duration. Similarly, this analysis can also be done for horizontal error, and other conflicting objectives.

- (iii) On the curve of non-dominated front, where no data are available, indicates infeasible parameter space i.e. all constraints are not satisfied. Using this information, a flight planner can visualize the available infeasible zones in the parameter space. For example, Figure 4 shows that an altimetric error in LiDAR data in the range of 8.04-8.06 cm, under the current set up of the constraints of the problem, cannot be achieved. Similarly, Figure 3 demonstrates that a planimetric error in the range of 13.2-14.2 cm cannot be achieved for the specifications of problem P2 because all active constraints are not satisfied for this range of planimetric errors. This information is also useful for deciding the limits of a conflicting variable in a specific range in single objective optimization. Similar inferences can be made with Figures 5 to 6 for problem P4.
- (iv) It should be noted that the multi-objective optimization demonstrates the variation between two conflicting objectives and thus a decision should not be made about the other objectives. With two particular objectives, the variations of remaining objectives are not considered. For example, as the flight duration and altimetric error are considered two objectives, the multi-objective optimization by NSGA-II code will show the variation of these two variables only as shown in Figure 4 (and 6). Therefore, as discussed earlier, a decision that fixes the values of these objectives using Figure 4 (and 6) can be made. However, by multi-objective optimization, any one conflicting objective with respect to flight duration can be considered for decision making. Therefore, multi-objective optimization is not a substitute of the single objective optimization but both optimization techniques complement each other.

## 7. Conclusions

This paper addresses various processes of the GA (e.g. variable handling, sampling, elite preservations, and parameter space *niching*) and their configurations (or algorithms). Further, the paper successfully outlined a step-by-step procedure to implement the developed algorithms. In order to test the algorithm, it is implemented on a complicated

four variants of optimization problem of flight planning for airborne LiDAR data acquisition. Four variants of the flight planning problem consist of different number of constraints. Performance of the algorithms are analyzed by consistency and convergence criteria using various statistical measures, like minimum, maximum, average and standard deviation of fitness function over multiple runs. Using a deductive approach, better algorithms are developed to solve a complicated single and multi-objective optimization version of the flight planning problem. It is noticed that continuous variables of optimization problem, initialized by Latin hypercube sampling, elite preservation by BRCR, and without parameter-space *niching* successfully detects the minimum in most runs. Moreover, as GA is least expected to show the biased behavior, the parameter space *niching* should not be attempted at first. Before applying the parameter space *niching* for single objective problems, it is recommended to exhaust all other possibilities of configuration of parameters of GA. Multi-objective optimization by NSGA-II code of flight planning problem provided the trade-off between the conflicting objectives (i.e. flight duration against planimetric and altimetric errors in LiDAR data). This case study remains as a testimony to developing efficient customized single and multi-objective optimization algorithms for solving real-world problems.

### **Acknowledgements**

Authors are thankful to Varun Jindal and Ashutosh for helping in development of physical model of flight planning problem.

### **References**

- [1] Goldberg, D.E., 1989. A Gentle Introduction to Genetic Algorithms, in *Genetic Algorithms in Search, Optimization, and Machine Learning*. Pearson Education Asia, Delhi (India), pp 1-25.
- [2] Dashora, A., 2012. *PhD Dissertation: Optimization System for Flight Planning for Airborne LiDAR Data Acquisition*, Indian Institute of Technology Kanpur, Kanpur (India), 216 pages.
- [3] Dashora, A. and Lohani, B., 2013. Turning Time Calculation for Airborne Surveys, *KanGAL Report No 2013010*, Indian Institute of Technology Kanpur, Kanpur (India).  
URL: <http://www.iitk.ac.in/kangal/reports.shtml> (last accessed May 26, 2013)
- [4] Dashora, A. and Lohani, B., 2013. Calculation of Error Propagated in Airborne LiDAR Data, *KanGAL Report No 2013011*, Indian Institute of Technology Kanpur, Kanpur (India).  
URL: <http://www.iitk.ac.in/kangal/reports.shtml> (last accessed May 26, 2013)

- [5] Deb, K., 2000. An Efficient Constraint Handling Method for Genetic Algorithms, *Computer Methods in Applied Mechanics and Engineering*, Vol. 186(2-4), pp 311–338.
- [6] Deb, K. and Goyal, M., 1996. A Combined Genetic Adaptive Search (GeneAS) for Engineering Design, *Computer Science and Informatics*, Vol. 26(4), pp 30–45.
- [7] Devay, K.R., 2008. Latin Hypercube Sampling and Pattern Search in Magnetic Field Optimization Problems, *IEEE Transactions on Magnetics*, Vol. 44(6), pp 974-977.
- [8] Deutsch, J.L. and Deutsch, C.V., 2012. Latin Hypercube Sampling with Multidimensional Uniformity, *Journal of Statistical Planning and Inference*, Vol. 142, pp 763-772.
- [9] McKay, M. D., Beckman, R.J. and Conover, W.J., 1979. A Comparison of Three Methods for Selecting Values of Input Variables in the Analysis of Output from a Computer, *Technometrics*, Vol 21(2), pp 239-245.
- [10] Hess, S., Train, K.E. and Polak, J.W., 2006. On the Use of a Modified Latin Hypercube Sampling (MLHS) Method in the Estimation of a Mixed Logit Model for Vehicle Choice, *Transportation Research Part B* 40, pp 147–163.
- [11] Tong, 2006. Tong, C., 2006. Refinement Strategies for Stratified Sampling Methods, *Reliability Engineering and System Safety*, Vol. 91, pp 1257–1265.
- [12] Petelet, M., Iooss, B., Asserin, O. and Loredo, A., 2010. Latin Hypercube Sampling with Inequality Constraints, *Advances in Statistical Analysis*, Vol. 94, pp 325-339.
- [13] Sallaberry, J., Helton, J.C. and Hora, S.C., 2006. Extension of Latin Hypercube Sampling with Correlated Variables, *Sandia Report No. 'SAND2006-6135'*, Sandia National Laboratories, United States Department of Energy, Albuquerque, New Mexico (USA), 48 pages.  
URL: <http://dakota.sandia.gov/papers/IncrMLHS.pdf> (last accessed September 7, 2012)
- [14] Durstenfeld, R., 1964. Algorithm 235: Random Permutation, *Communications of ACM*, Vol. 7(7), page 420.
- [15] Deb, K. 2005. A Population-Based Algorithm-Generator for Real-Parameter Optimization, in F. Herrera and M. Lozano (eds.), Special Issue on "Real Coded Genetic Algorithms: Foundations, Models and Operators", *Soft Computing Journal*, Vol. 9, pp 236-253.
- [16] Goldberg, D.E. and Richardson, J., 1987. Genetic Algorithms for Sharing for Multimodal Function Optimization, *Proceedings of the 2<sup>nd</sup> International Conference on Genetic Algorithms*, Lawrence Erlbaum Associates, pp 41-49.
- [17] Deb, K., 2001. *Multi-Objective Optimization using Evolutionary Algorithms*, John Wiley & Sons Inc., Chichester (UK), 515 pages.
- [18] Deb, K., Pratap, A., Agarwal, S., and Meyarivan, T., 2002. A Fast and Elitist Multi-objective Genetic Algorithm: NSGA-II, *IEEE Transactions on Evolutionary Computation*, Vol. 6(2), pp 182-197.
- [19] Deb, K., and Kumar, A., 1995. Real-coded Genetic Algorithms with Simulated Binary Crossover: Studies on Multi-modal and Multi-objective Problems, *Complex Systems*, Vol. 9, pp 431-454.
- [20] Deb, K., and Deb, D., 2012. Analyzing Mutation Schemes for Real-Parameter Genetic Algorithms, *KanGAL Report Number 2012016*, Indian Institute of Technology Kanpur, Kanpur (India).  
URL: <http://www.iitk.ac.in/kangal/reports.shtml> (last accessed May 26, 2013)

- [21] Deb, K., 1995. Ch-6: Nontraditional Optimization Algorithms (pp 290-359), in *Optimization for Engineering Design: Algorithms and Examples*, PHI Learning Pvt. Limited, New Delhi (India), 10th print, 396 pages.
- [22] Mavrotas, G., 2009. Effective Implementation of the E-Constraint Method in Multi-Objective Mathematical Programming Problems, *Applied Mathematics and Computation*, Vol. 213, pp 455-465.